

AIP Conference Proceedings



Volume 2836

THERMOFLUID XII The 12th International Conference on Thermofluids 2021

Yogyakarta, Indonesia • 10–11 November 2021

Editors • Hifni Mukhtar Ariyadi, Indarto, Samsul Kamal,
Harwin Saptoadi and Deendarlianto



Available Online: pubs.aip.org/aip/acp

RESEARCH ARTICLE | APRIL 03 2024

Preface of the 12th International Conference on Thermofluids 2021

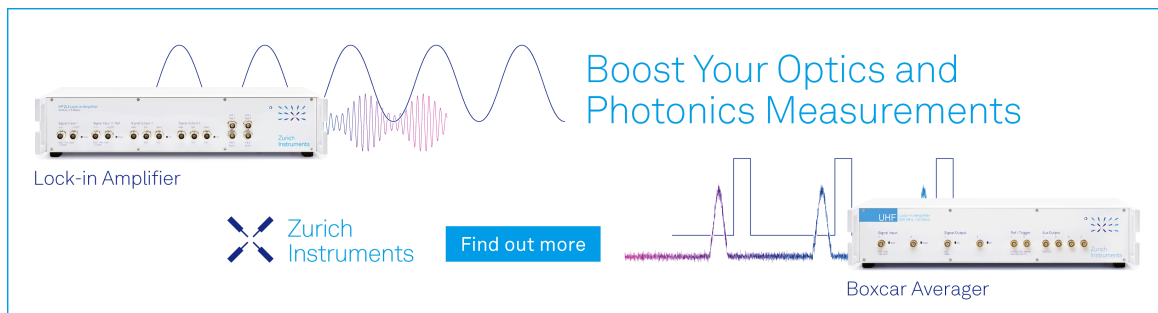
 Check for updates

AIP Conf. Proc. 2836, 010001 (2024)


<https://doi.org/10.1063/1.2022547>



Boost Your Optics and Photonics Measurements



Lock-in Amplifier



[Find out more](#)

Boxcar Averager

Preface of the 12th International Conference on Thermofluids 2021

The 12th International Conference on Thermofluids 2021 is the 12th series of annual Thermofluid conference held by the Department of Mechanical and Industrial Engineering of Universitas Gadjah Mada on 10th -11th November 2021. This conference is also the 2nd series of the Thermofluid held online due to the ongoing COVID-19 pandemic. We hope it does not detract the value, purpose, and the quality of the event.

In this conference, we are expecting that national and international researchers, engineers, and academia share and disseminate their recent development status of researches, especially in the field of thermal, fluid, and energy engineering to advance future clean energy solutions as we are at a critical moment where clean energy must advance at a much more rapid pace to prevent the lasting impacts of climate change.

On behalf of the committee, I would like to express our outmost gratitude to all who have made the 12th International Conference on Thermofluids 2021. We have received numerous invaluable contributions for this conference encompassing research and developments in Fluid Dynamics, Multiphase Flow, Fuel Technology, Thermodynamics, Energy Conversion, Fluid Structure Interaction, Heat and Mass Transfer and Phase Change, Renewable Energy and Energy Harvesting, Combustion and Automotive Engineering. We thank all the authors, reviewers, moderators, and participants for their contributions.

I would also like to express our appreciation to our distinguished keynote speakers: Prof. Deendarlianto from Universitas Gadjah Mada, Prof. Kiyoshi Saito from Waseda University, Prof. Michael Beckmann from Technical University Dresden, Assoc.Prof. Agus Pulung Sasmito from the University of Montreal, Prof. Alberto Coronas from Rovira I Virgili University, Dr. Dadan Kusdiana from the Directorate General of New Renewable Energy and Energy Conservation, Ministry of Energy and Mineral Resources, and Dr. Djoko Hendratto from The Environmental Fund Management Agency.

Finally, this conference would not be possible without the tireless efforts of the committee members who have worked hard as a team. We hope this event will further stimulate research in thermal, fluid and energy engineering.

Dr. Hifni Mukhtar Ariyadi

Organizing Committee Chairman

RESEARCH ARTICLE | APRIL 03 2024

Committee: 12th International Conference on Thermofluids 2021

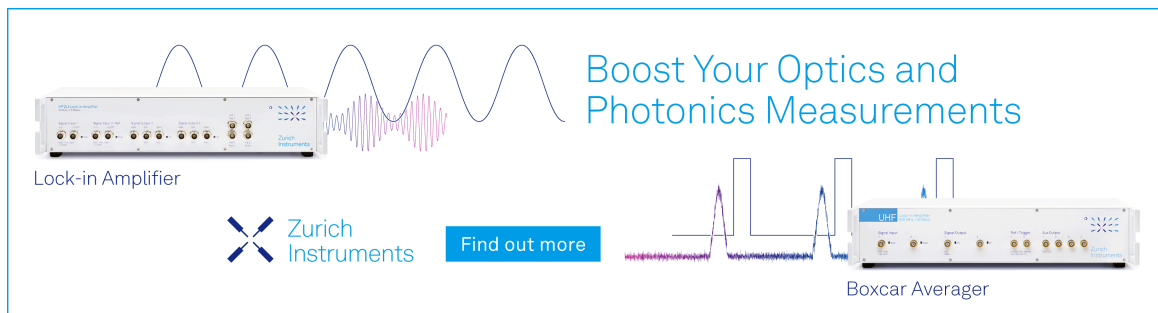
 Check for updates

AIP Conf. Proc. 2836, 010002 (2024)


<https://doi.org/10.1063/1.2025493>



Boost Your Optics and Photonics Measurements



Lock-in Amplifier



Find out more

Boxcar Averager

CONFERENCE COMMITTEE

Scientific and Steering Committee

Prof. Indarto (Universitas Gadjah Mada, Indonesia)
Prof. Samsul Kamal (Universitas Gadjah Mada, Indonesia)
Prof. Harwin Saptoadi (Universitas Gadjah Mada, Indonesia)
Assoc. Prof. Chong Wen Tong (University of Malaya, Malaysia)
Dr.-Ing. Marco Jose da Silva (Universidade Tecnológica Federal do Paraná, Brazil)
Assoc. Prof. Leong Kai Choong (Nanyang Technological University, Singapore)
Assoc. Prof. Agus Pulung Sasmito (McGill University, Canada)
Prof. Tetsuya Suekane (Tokyo Institute of Technology, Japan)
Prof. Alberto Coronas (Rovira I Virgili University, Spain)
Budi Hartono, Ph.D. (Universitas Gadjah Mada)
Dr. Adhika Widyaparaga (Universitas Gadjah Mada)
Joko Waluyo, Ph.D. (Universitas Gadjah Mada)
Prof. Deendarlianto (Universitas Gadjah Mada)
Dr. Jayan Sentanuhady (Universitas Gadjah Mada)

Organizing Committee

Conference Chair

Dr. Hifni Mukhtar Ariyadi

Vice-Chair

Ryan A. Putra, M.Eng.

Secretary and Treasury

Willie Prasadha, S.T., M.Eng.

Publication and Proceeding

Dr. Hifni Mukhtar Ariyadi

Ryan A. Putra, M.Eng.

Willie Prasadha, M.Eng.

Arif Widyatama, M.Eng

RESEARCH ARTICLE | APRIL 03 2024

Editorial Boards: 12th International Conference on Thermofluids 2021

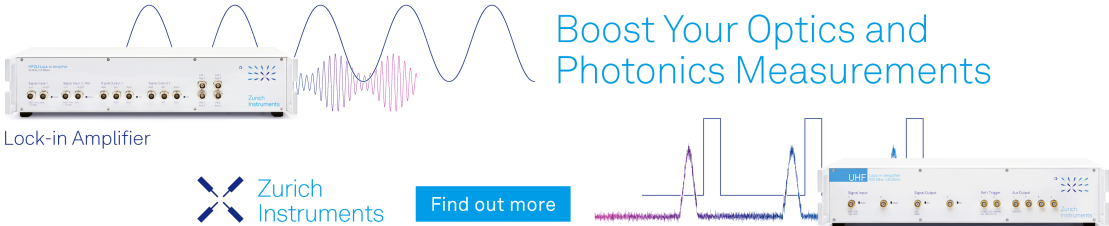
 Check for updates

AIP Conf. Proc. 2836, 010003 (2024)


<https://doi.org/10.1063/1.20025494>



Boost Your Optics and Photonics Measurements



Lock-in Amplifier



[Find out more](#)

Boxcar Averager

EDITORIAL BOARDS

Editor In Chief

Dr. Hifni Mukhtar Ariyadi (Universitas Gadjah Mada, Indonesia)

Associate Editors

Prof. Indarto (Universitas Gadjah Mada, Indonesia)

Prof. Samsul Kamal (Universitas Gadjah Mada, Indonesia)

Prof. Harwin Saptoadi (Universitas Gadjah Mada, Indonesia)

Prof. Deendarlianto (Universitas Gadjah Mada)

Advisory Editors

Assoc. Prof. Chong Wen Tong (University of Malaya, Malaysia)

Dr.-Ing. Marco Jose da Silva (Universidade Tecnológica Federal do Paraná, Brazil)

Assoc. Prof. Leong Kai Choong (Nanyang Technological University, Singapore)

Assoc. Prof. Agus Pulung Sasmito (McGill University, Canada)

Prof. Tetsuya Suekane (Tokyo Institute of Technology, Japan)

Prof. Alberto Coronas (Rovira I Virgili University, Spain)

Prof. Budi Hartono (Universitas Gadjah Mada, Indonesia)

Dr. Adhika Widyaparaga (Universitas Gadjah Mada, Indonesia)

Issues

Select Decade 2020 ▾

Select Year 2024 ▾

Issue 3 April - Volume 2836, Issue 1 ▾

PRELIMINARY

Preface of the 12th International Conference on Thermofluids 2021 FREE

AIP Conf. Proc. 2836, 010001 (2024) <https://doi.org/10.1063/12.0022547>

[View article](#)

[PDF](#)

Committee: 12th International Conference on Thermofluids 2021 FREE

AIP Conf. Proc. 2836, 010002 (2024) <https://doi.org/10.1063/12.0025493>

[View article](#)

[PDF](#)

Editorial Boards: 12th International Conference on Thermofluids 2021 FREE

AIP Conf. Proc. 2836, 010003 (2024) <https://doi.org/10.1063/12.0025494>

[View article](#)

[PDF](#)

COMBUSTION AND AUTOMOTIVE ENGINEERING

The study of swirl vanes blade amount effect on the visualization and temperature distribution of co-flow diffusion flame FREE

[Radissa Dzaky Issafira](#); [Widya Wijayanti](#); [Luluk Edahwati](#); [Wahyu Dwi Lestari](#); [Ahmad Khairul Faizin](#); [Wiliandi Saputro](#)

[Abstract](#) 

[View article](#)

 [PDF](#)

ENERGY CARRIER AND STORAGE

Study of loop heat pipe prototype technology as a passive cooling system in nuclear reactors based on technology audit **FREE**

[Sigit Santosa](#); [M. Hadi Kusuma](#); [Wegie Ruslan](#); [Khusnul Khotimah](#); [Giarno](#)

AIP Conf. Proc. 2836, 030001 (2024) <https://doi.org/10.1063/5.0206264>

[Abstract](#) 

[View article](#)

 [PDF](#)

FLUID DYNAMICS

Large eddy simulation (LES) unsteady flow study of centrifugal compressor using OpenFOAM **FREE**

[Caesar Wiratama](#)

AIP Conf. Proc. 2836, 040001 (2024) <https://doi.org/10.1063/5.0207352>

[Abstract](#) 

[View article](#)

 [PDF](#)

Computational modelling of Non-Newtonian blood flow through carotid artery bifurcation **FREE**

[Ahmad Khairul Faizin](#); [Wiliandi Saputro](#); [Radissa Dzaky Issafira](#); [N. Adyono](#); [Tria Puspa Sari](#); [W. D. Lestari](#); [Luluk Edahwati](#)

AIP Conf. Proc. 2836, 040002 (2024) <https://doi.org/10.1063/5.0188374>

[Abstract](#) 

[View article](#)

 [PDF](#)

A fourth-order compact finite difference method for solving incompressible flows **FREE**

[Caesar Ondolan Harahap](#); [Christopher Leonard](#)

AIP Conf. Proc. 2836, 040003 (2024) <https://doi.org/10.1063/5.0188440>

[Abstract](#) 

[View article](#)

 [PDF](#)

Modelling and simulation of a single-zone highly occupied indoor space to minimize aerosol exposure and energy consumption of HVAC systems **FREE**

Fahreza Ramadhan; Dereje S. Ayou; Juan Prieto; Alberto Coronas

AIP Conf. Proc. 2836, 040004 (2024) <https://doi.org/10.1063/5.0188283>

Abstract ▾

View article

 PDF

Computational fluid dynamics of the free water flow through t-he water turbine adapted goose foot **FREE**

Retno Wulandari; Suprayitno Suprayitno; Yuli Astuti; Pingkan Sihassaleh; Abdurrahman Zaqi Habibie

AIP Conf. Proc. 2836, 040005 (2024) <https://doi.org/10.1063/5.0189926>

Abstract ▾

View article

 PDF

Numerical simulation the effects of flow diverter configuration on flue gas flow characteristics in HRSG **FREE**

Atanasius Hardito Putro; Joko Waluyo

AIP Conf. Proc. 2836, 040006 (2024) <https://doi.org/10.1063/5.0207268>

Abstract ▾

View article

 PDF

Use of regular patterns-based background oriented schlieren imaging and digital image correlation for visualization of convective airflow **FREE**

Margi Sasono; Setyawan P. Sakti; Johan E. Noor; Hariyadi Soetedjo

AIP Conf. Proc. 2836, 040007 (2024) <https://doi.org/10.1063/5.0188501>

Abstract ▾

View article

 PDF

Thermal hydraulic analysis of the Bandung Triga 2000 research reactor **FREE**

P. Basuki; E. Umar

AIP Conf. Proc. 2836, 040008 (2024) <https://doi.org/10.1063/5.0205674>

Abstract ▾

View article

 PDF

Performance analysis off-design centrifugal compressor performance through numerical simulation FREE

Joko Waluyo; Charottama Daffa Hardanendra; Atanasius Hardito Putro

AIP Conf. Proc. 2836, 040009 (2024) <https://doi.org/10.1063/5.0207269>

Abstract 

View article

 PDF

Performance comparison of centrifugal compressor in variation impeller outlet blade angle through numerical simulation FREE

Joko Waluyo; Hafid Nur Shafuat; Atanasius Hardito Putro

AIP Conf. Proc. 2836, 040010 (2024) <https://doi.org/10.1063/5.0207270>

Abstract 

View article

 PDF

FLUID STRUCTURE INTERACTION

Cassava starch granule breaking enhancement by sequential high shear mixing and sonication FREE

Sumarno; Prida Novarita Trisanti; Bramantyo Airlangga; Febriyati Puspasari

AIP Conf. Proc. 2836, 050001 (2024) <https://doi.org/10.1063/5.0188504>

Abstract 

View article

 PDF

In situ particles-liquid imaging in centrifugal fields by improved ANN-SPH-DEM into linear sensor-type wireless electrical resistance tomography (*ISWERT*) FREE

Kota Kimura; Yosephus Ardean Kurnianto Prayitno; Prima Asmara Sejati; Daisuke Kawashima; Masahiro Takei

AIP Conf. Proc. 2836, 050002 (2024) <https://doi.org/10.1063/5.0189210>

Abstract 

View article

 PDF

FUEL TECHNOLOGY

Simulation of coconut shell combustion in a grate-fired furnace using distributed pyrolysis products model **FREE**

Muhammad Y. Habibi; Maulana G. Nugraha; Muslikhin Hidayat; Harwin Saptoadi

AIP Conf. Proc. 2836, 060001 (2024) <https://doi.org/10.1063/5.0207275>

Abstract ▾

View article

 PDF

RENEWABLE ENERGY AND ENERGY HARVESTING

Oil extraction from kapok (*Ceiba pentandra*) and beauty leaf (*Calophyllum inophyllum*) seeds with variations of extraction method and pre-treatment **FREE**

Yasmin Zulfati Yusrina; Yuli Setyo Indartono; Tirto Prakoso

AIP Conf. Proc. 2836, 070001 (2024) <https://doi.org/10.1063/5.0207503>

Abstract ▾

View article

 PDF

Condensate production rate from residential air conditioning at different outdoor air conditions **FREE**

Kasni Sumeru; Triaji Pangripto; Afif Miftakh Hafidzudin; Ryan Ferdiansyah; Mohamad Firdaus bin Sukri

AIP Conf. Proc. 2836, 070002 (2024) <https://doi.org/10.1063/5.0188790>

Abstract ▾

View article

 PDF

The hydraulic retention time (HRT) control upon palm oil mill effluent (POME) treatment by bio-CSTR 1 m³ **FREE**

Galuh Wirama Murti; Joni Prasetyo; Arya Bhaskara Adiprabowo; Zulaicha Dwi Hastuti; Nurdiah Rahmawati; Atti Solihah; Septina Is Heriyanti; Era Restu Finalis; Tyas Puspita Rini; Novio Valentino; Samuel Pati Senda

AIP Conf. Proc. 2836, 070003 (2024) <https://doi.org/10.1063/5.0206013>

Abstract ▾

View article

 PDF

Enhancing the microalgae *Nannochloropsis* sp. harvesting by chitosan-based flocculation-sedimentation for biofuel production **FREE**

Yano Surya Pradana; Yuni Kusumastuti; Nur Rofiqoh Eviana Putri; Aitia Mulyawati Widiyannita; Devi Swasti Prabasiwi; Arina Nur Fitri Fadhila; Eko Agus Suyono

AIP Conf. Proc. 2836, 070004 (2024) <https://doi.org/10.1063/5.0188425>

Abstract ▾

View article

 PDF

Techno-Economic assessment of mobile rice husk gasifier as bioenergy technology integration in Indonesia **FREE**

Yohanes Bobby Sanjaya; Hafif Dafiqurrohman; Yuswan Muharam; Adi Surjosatyo

AIP Conf. Proc. 2836, 070005 (2024) <https://doi.org/10.1063/5.0205826>

Abstract ▾

View article

 PDF

Performance analyse of solar rooftop at Medan city in Indonesia **FREE**

Immanuelta Sitepu; Farel H. Napitupulu; Himsar Ambarita

AIP Conf. Proc. 2836, 070006 (2024) <https://doi.org/10.1063/5.0188337>

Abstract ▾

View article

 PDF

Investigation of variation of inner blade height of the five blade runner on the kaplan turbine against turbine power **FREE**

Sirojuddin; Tony; N. S. Dewi; A. A. Zahara; A. A. Jumhur

AIP Conf. Proc. 2836, 070007 (2024) <https://doi.org/10.1063/5.0195100>

Abstract ▾

View article

 PDF

The effect of the number of blades on vortex turbine performance **FREE**

Rayno Luther Hasiholan; Ari Prasetyo; Dominicus Danardono Dwi Prija Tjahjana; Syamsul Hadi

AIP Conf. Proc. 2836, 070008 (2024) <https://doi.org/10.1063/5.0188380>

Abstract ▾

View article

 PDF

Flow simulation on a vortex turbine using CFD with various outlet diameter sizes **FREE**

[Idham Kamil](#); [Budiman Y. Simbolon](#); [Iman Telaumbanua](#); [Burhan Hafid](#); [Tulus B. Sitorus](#); [Farel H. Napitupulu](#); [Himsar Ambarita](#)

AIP Conf. Proc. 2836, 070009 (2024) <https://doi.org/10.1063/5.0188338>

[Abstract](#) ▾

[View article](#)

[PDF](#)

HEAT - MASS TRANSFER AND PHASE CHANGE

Determining the thermal conductivity of natural fibres with axial flow method **FREE**

[Ali Gunawan](#); [Nandy Putra](#); [Evi Sofia](#); [Ragil Sukamo](#)

AIP Conf. Proc. 2836, 080001 (2024) <https://doi.org/10.1063/5.0188599>

[Abstract](#) ▾

[View article](#)

[PDF](#)

Steam generator cooling post LOCA with ECCS failure in NuScale reactor using RELAP5 **FREE**

[Susyadi](#); [Raldi Artono Koestoer](#); [Nandy Putra](#); [Mulya Juarsa](#)

AIP Conf. Proc. 2836, 080002 (2024) <https://doi.org/10.1063/5.0205743>

[Abstract](#) ▾

[View article](#)

[PDF](#)

Thermal performance and properties analysis of a building envelope integrated with phase change material for energy conservation in a tropical climate region **FREE**

[Imansyah Ibnu Hakim](#); [Reza Edriawan](#); [Nandy Putra](#)

AIP Conf. Proc. 2836, 080003 (2024) <https://doi.org/10.1063/5.0188417>

[Abstract](#) ▾

[View article](#)

[PDF](#)

Simulation of temperature and air flow distribution in coffee drying chamber using low enthalpy geothermal energy resource with thermosiphon technology **FREE**

[Imansyah Ibnu Hakim](#); [Irene Deby Palupi](#); [Nandy Putra](#)

[Abstract](#) 

[View article](#)

 [PDF](#)

The rate of internal energy changes on u-shape heat exchanger inside water cooling tank of FASSIP-02 test loop base on variation temperature in heating area **FREE**

[Giarno Giarno](#); [Dedy Haryanto](#); [Gregorius Kusnugroho](#); [Ainur Rosidi](#); [Adhika Pamungkas](#); [Mulya Juarsa](#)

AIP Conf. Proc. 2836, 080005 (2024) <https://doi.org/10.1063/5.0205577>

[Abstract](#) 

[View article](#)

 [PDF](#)

Sea-water ice slurry generator for 25 GT fishing boat with 5.17 tons of fish **FREE**

[Yafi Rahmad Oktafian](#); [Agus S. Pamitran](#)

AIP Conf. Proc. 2836, 080006 (2024) <https://doi.org/10.1063/5.0188318>

[Abstract](#) 

[View article](#)

 [PDF](#)

Study of adiabatic length effect on the thermal performance of the wick-less straight heat pipe using RELAP5 **FREE**

[Surip Widodo](#); [Nandy Putra](#); [Anhar Riza Antariksawan](#); [Mukhsinun Hadi Kusuma](#); [Mulya Juarsa](#)

AIP Conf. Proc. 2836, 080007 (2024) <https://doi.org/10.1063/5.0205742>

[Abstract](#) 

[View article](#)

 [PDF](#)

A fourth-order compact finite difference method for solving natural convection in rectangular enclosures **FREE**

[Christopher Leonard](#); [Caesar Ondolan Harahap](#)

AIP Conf. Proc. 2836, 080008 (2024) <https://doi.org/10.1063/5.0188442>

[Abstract](#) 

[View article](#)

 [PDF](#)

Effect of an evaporator pipe length on the water production of a small air-water harvester FREE

Mirmanto Mirmanto; Syahrul Syahrul; Agung Tri Wijayanta; Ahmad Faroni; Alvin Azari; Ida Afriani; Dini Dwi Lestari; Abdulloh Habib

AIP Conf. Proc. 2836, 080009 (2024) <https://doi.org/10.1063/5.0207342>

[Abstract](#) 

[View article](#)

 [PDF](#)

MULTIPHASE FLOW

Review paper of two-phase flow boiling pressure drop in propane refrigeration system FREE

Edo Widi Virgian; Agus S. Pamitran

AIP Conf. Proc. 2836, 090001 (2024) <https://doi.org/10.1063/5.0188320>

[Abstract](#) 

[View article](#)

 [PDF](#)

Numerical study of high viscous oil-water multiphase flows in a horizontal pipe using the AIAD model FREE

Bahrul Jalaali; Okto Dinaryanto; Muhammad Ridlo Erdata Nasution

AIP Conf. Proc. 2836, 090002 (2024) <https://doi.org/10.1063/5.0188696>

[Abstract](#) 

[View article](#)

 [PDF](#)

Stochastic and wavelet analysis towards liquid film thickness fluctuations during countercurrent flow limitation on a complex geometry by using image processing FREE

Akhliisa Nadiantya Aji Nugroho; Deendarlianto; Indarto; Achilleus Hermawan Astyanto

AIP Conf. Proc. 2836, 090003 (2024) <https://doi.org/10.1063/5.0207224>

[Abstract](#) 

[View article](#)

 [PDF](#)

Prediction of void fraction of R290 in a horizontal condenser FREE

Windy H. Mitrakusuma; Andriyanto Setyawan

AIP Conf. Proc. 2836, 090004 (2024) <https://doi.org/10.1063/5.0188722>

[Abstract](#) 

[View article](#)

 [PDF](#)

The effect of the liquid viscosity on the liquid film thickness and wave frequency of the gas-liquid stratified co-current flow in horizontal pipes **FREE**

[Setya Wijayanta](#); [Indarto](#); [Deendarlianto](#); [Christoforus Yacob Sianipar](#)

AIP Conf. Proc. 2836, 090005 (2024) <https://doi.org/10.1063/5.0188647>

[Abstract](#) 

[View article](#)

 [PDF](#)

Effect of evaporating temperature on vapor quality and void fraction of R454B in horizontal evaporator **FREE**

[Windy H. Mitrakusuma](#); [Apip Badarudin](#); [Andriyanto Setyawan](#)

AIP Conf. Proc. 2836, 090006 (2024) <https://doi.org/10.1063/5.0188723>

[Abstract](#) 

[View article](#)

 [PDF](#)

Two phase flow pressure drop measurement analysis in a horizontal rectangular minichannel T-junction **FREE**

[Untung Surya Dharma](#); [Deendarlianto](#); [Indarto](#)

AIP Conf. Proc. 2836, 090007 (2024) <https://doi.org/10.1063/5.0207223>

[Abstract](#) 

[View article](#)

 [PDF](#)

Experimental study of the visualization of bubble breaking mechanism on the swirl type MBG output channel **FREE**

[Drajat Indah Mawarni](#); [Indarto](#); [Deendarlianto](#)

AIP Conf. Proc. 2836, 090008 (2024) <https://doi.org/10.1063/5.0188339>

[Abstract](#) 

[View article](#)

 [PDF](#)

Enhanced oil recovery by using polymer flooding with shear-thinning property and in-situ chemical reaction **FREE**

[Sotheavuth Sin](#); [Weicen Wang](#); [Yun She](#); [Anindityo Patmonoaji](#); [Tetsuya Suekane](#)

AIP Conf. Proc. 2836, 090009 (2024) <https://doi.org/10.1063/5.0188875>

[Abstract](#) 

[View article](#)

 [PDF](#)

THERMODYNAMICS AND ENERGY CONVERSION

Simulation of the effect of fan cooling tower variations on the performance and energy consumption of water cooled chiller with R-514a as refrigerant **FREE**

[Ade Suryatman Margana](#); [Susilawati](#); [Fariyani](#)

AIP Conf. Proc. 2836, 100001 (2024) <https://doi.org/10.1063/5.0189060>

[Abstract](#) 

[View article](#)

 [PDF](#)

Effect of refrigerant charge on the performance and environmental footprint of R32 heat pump water heater **FREE**

[Muhamad Yulianto](#); [Niccolo Giannetti](#); [Yoichi Miyaoka](#); [Zheng Ge](#); [Takashi Tsuchino](#); [Masakazu Urakawa](#); [Shigeru Taira](#); [Jongsoo Jeong](#); [Kiyoshi Saito](#)

AIP Conf. Proc. 2836, 100002 (2024) <https://doi.org/10.1063/5.0207267>

[Abstract](#) 

[View article](#)

 [PDF](#)

Preliminary study of integrated bottoming binary cycle and electrolysis unit to utilize separated brine at Ulubelu geothermal power plant for green hydrogen production **FREE**

[Vincentius Adven Brilian](#); [Fikri Muhammad Akbar](#); [Akmal Irfan Majid](#); [Khasani](#); [Mohamad Husni Mubarak](#)

AIP Conf. Proc. 2836, 100003 (2024) <https://doi.org/10.1063/5.0188311>

[Abstract](#) 

[View article](#)

 [PDF](#)

The novel design for cooling system of greenhouse **FREE**

[Amelia Sugondo](#); [Ekadewi A. Handoyo](#); [Guntar Henjaya](#)

AIP Conf. Proc. 2836, 100004 (2024) <https://doi.org/10.1063/5.0188395>

[Abstract](#) 

[View article](#)

 [PDF](#)

Computational study on liquid-liquid extraction of formic acid using methyl isobutyl ketone solvent with the aid of biological buffer as green auxiliary agent **FREE**

Saidah Altway; Serli Dwi Rahayu; Muhammad Irvansyah; Soeprijanto; Daril Ridho Zuchrillah; Ardila Hayu Tiwikrama

AIP Conf. Proc. 2836, 100005 (2024) <https://doi.org/10.1063/5.0188792>

Abstract 

View article

 PDF

RESEARCH ARTICLE | APRIL 03 2024

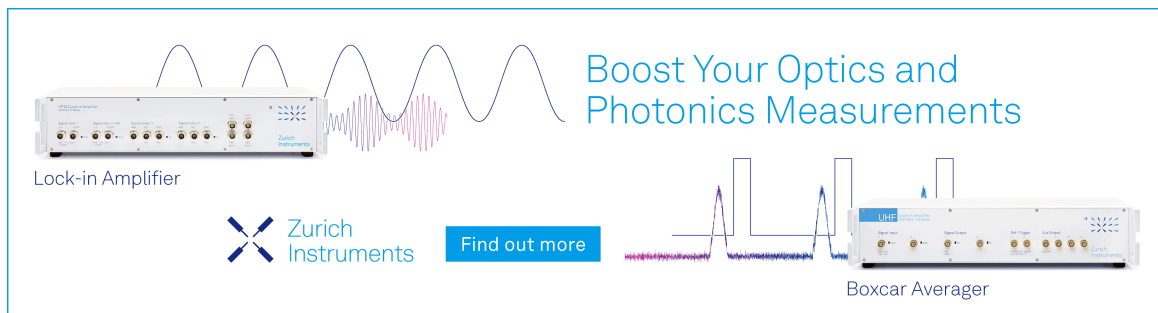
Stochastic and wavelet analysis towards liquid film thickness fluctuations during countercurrent flow limitation on a complex geometry by using image processing

Akhliisa Nadiantya Aji Nugroho , Deendarlianto; Indarto; Achilleus Hermawan Astyanto

 Check for updates


AIP Conf. Proc. 2836, 090003 (2024)

<https://doi.org/10.1063/5.0207224>



Boost Your Optics and Photonics Measurements

Lock-in Amplifier

 Zurich Instruments

[Find out more](#)

Boxcar Averager

Stochastic and Wavelet Analysis towards Liquid Film Thickness Fluctuations During Countercurrent Flow Limitation on A Complex Geometry by Using Image Processing

Akhliisa Nadiantya Aji Nugroho^{1, a)}, Deendarlianto^{1, b)}, Indarto^{1, c)}, and Achilleus Hermawan Astyanto^{1, 2, d)}

¹Department of Mechanical and Industrial Engineering, Universitas Gadjah Mada, Jl. grafika No 2 Kampus UGM, Yogyakarta 55281, Indonesia

²Department of Mechanical Engineering, Universitas Sanata Dharma, Kampus III USD, Yogyakarta 55282, Indonesia

Corresponding author: akhliisa.nadiantya.a@mail.ugm.ac.id^{a)}
deendarlianto@ugm.ac.id^{b)}
indarto@ugm.ac.id^{c)}
achil.herma@mail.ugm.ac.id^{d)}

Abstract. This study investigates the statistical characteristics of liquid film thickness fluctuations during countercurrent flow limitation on a complex geometry containing a horizontal and inclined pipe which are connected by an elbow. The fluctuation data are obtained by image processing technique which was applied towards high-quality images captured by a high-speed video recording. The result indicates that the thickening of the liquid triggers the liquid blockage that initiates flooding at the upper edge of the hydraulic jump. Moreover, the stochastic analysis reveals that the obtained data imply consistence trends across whole water discharge. Furthermore, it also shows a good agreement to the visual observations. Meanwhile, the wavelet analysis can distinguish energy fluctuations under different water discharges.

INTRODUCTION

A pressurized water reactor (PWR) is one of the most popular reactors to generate electricity through nuclear reaction. The reactor is operated at high pressure and temperature. In its reactor core, called the reactor pressure vessel (RPV), the operating pressure and temperature reach 15 MPa and 325 °C, respectively. The construction of the PWR reactor consists of three circuits loops, the primary circuit loop being the concern in this CCFL study. The primary circuit loop contains 3 main components; Reactor Pressure Vessel (RPV), Hot leg, and Steam generator (SG), RPV is connected to SG through a hot leg channel. The condensate water in the primary circuit is maintained at high pressure to increase the fluid boiling point and make the condensate water still in the liquid phase at high temperature circulation in primary circuit. The pressurized condensate water with high-temperature flows from the RPV to the SG, pressurized condensate water is used to generated superheated vapor in secondary circuit with heat transfer mechanism in SG.

Loss of cooling accident (LOCA) is a reactor nuclear accidental scenario, this accident scenario occurs when there is leakage on the primary circuit. The leakage in the primary circuit causes depressurization, and results the condensate water in RPV turns into a vapor phase. It further forms steam flows through the hot leg into the steam generator, the steam production increases alongside the time. When the steam flow rate through hot leg exceeds the limit, an amount of cooling water from the steam generator (SG) will be clogged in hot leg, some coolants are carried by the steam and flow back to the steam generator (SG). Consequently, the coolants flows to reactor core decreases, this phenomenon can lead core meltdown / nuclear accident.

Therefore, flooding is a complex physical phenomenon; it is always required to access information to enhance understanding of flooding phenomena. Wongwises (1996) performed a study on countercurrent flow limitation in a

horizontal and inclined pipe connected by an elbow. The length of the horizontal pipe is 1300 mm with a diameter of 64 mm. The bend has outer and inside curvature radii 60 mm and 135 mm. Here, the CCFL is divided into three regions. The first and third regions have a characteristic that airflow rate, which initiates the flooding, decreases with the increase of the water flow rate. In the second region, the airflow rate which initiates the flooding increases as the water flow rate increases. Moreover, Navarro (2005) investigated the effect of apparatus geometry configuration (pipe diameter, inclination angle, liquid holdup, liquid injected) and the liquid superficial velocity. When the water flow rate increases, the airflow required to initiate flooding decreases, but from flooding to zero liquid penetration, the airflow required remains constant when the water flow rate increases.

Deendarlianto et al. (2008) utilized a hot leg simulator with a rectangular cross sectional area model to conduct CCFL experiments. The rectangular channel section used 0.05 m x 0.25 m in dimension. The geometry was based on the German convoy PWR reactor at a scale of 1/3. A pressure chamber (TOPFLOW) was employed in the reactor simulator to regulate the reactor's working pressure. The flow behaviour in the test section is visualized using a high-speed camera. The flooding mechanism was identical to that described by Wongwises et al. (1996). Moreover, the Wallis parameter does not correlate with the pressure or working fluid types in this study. Furthermore, the countercurrent flow at low gas flow along the hot leg was also reviewed by Deendarlianto et al. (2012). Here, the pressure differences between the RPV and SG were low and progressively increased as gas flow rates increased. It is also noticed that the onset of flooding occurs when gas mass flow rates are equal to the liquid mass flow rate.

Al Issa and Macian (2011) analysed the visualization of flooding in a 1/3.9 reactor simulator with varying gas and liquid flow. This work obtained the visualization of initialization of flooding until the onset of flooding. Here, the gradual increase in gas flow distorts fluid flow and causes condensate water flow to partially or completely change direction (CCFL). Moreover, an experimental study of the mechanism of air-water flooding at a scale of 1/3.9 of the PWR hot leg was also extended Al Issa and Macian (2014). Four flooding areas based on the water's superficial velocity are established. Each flooding process begins with a small roll wave and progresses to a large roll wave, then slug flow. Flooding becomes more rapid as the superficial velocity the water increases.

Badarudin et al. (2016) performed a flooding and de-flooding investigation in 1/30 scale PWR reactor. A differential pressure transducer between SG and RPV was utilized to obtain the pressure fluctuation data during the onset of flooding. Here, a high-speed video camera with a frame rate of 60 fps also applied to capture the image. Furthermore, the liquid film thickness data were obtained by the image processing method. The CCFL experiment conducted by varying water and air superficial velocity. At low liquid superficial velocity Hydraulic jump and liquid blockage occurred near the bend, in other hand at medium and high liquid superficial velocities Hydraulic jump and liquid blockage occurred in the horizontal section of hot leg. Furthermore, Badarudin et al. (2018) using parallel wire sensor to identify thickness film characteristic in 1/30 scale PWR reactor, The liquid and gas superficial velocities (J_L and J_G) were varied. The onset of flooding was divided into three regions, the flow at first and third regions reaches the onset of flooding faster as the liquid flow rate increases. In a contrary, the flow in the second region reaches the onset of flooding faster as the liquid flow rate decreases. However, the study has not carried out the wavelet and stochastic analysis.

Rodrigues (2020) investigated the thickness of two-phase flow by utilizing a resistive sensor positioned on a horizontal pipe to determine the film thickness characteristic and the properties of power spectrum density (PSD) function. Two distinct sorts of probability density function (PDF) curves based on the void fraction value are discovered. Here, the void fraction affects the shape of the PSD. In this study, when the superficial velocity of water increases while maintaining the superficial gas velocity constant, the left PDF curve increases while the void fraction remains constant. When the superficial gas velocity increases while maintaining the superficial flow velocity constant, the value of the PDF curve on the right increases due to an increase in the void percentage. The effect frequency distribution the occurrence of slug flow also described. When the superficial velocity of water is varied, clear findings may be achieved, whereas increase in the superficial velocity of water results in a flatter PDF curve and a more extensive frequency range.

Jana (2006) investigated the interaction of two phases of oil and water in a vertical pipe. The study varied the liquid superficial velocity in oil and water between 0.05 and 1.5 m/s, respectively. The speed of the kerosene was varied under a constant water velocity. The results indicate that when the oil velocity is increased, some visualizations on the channel show the appearance of an oil plug. Furthermore, the decrease of v/v_{max} results the skewness also shifts to the positive direction while the oil flow increases again, indicating that the oil flow condition has begun to dominate the pipeline. This study can determine the flow characteristics by observing the PDF curve and the PDF curve shifts. The present study demonstrates that when the oil flow is more dominant, the skewness of the PDF curve shifts to the right, and the value of v/v_{max} decreases.

EXPERIMENTAL APPARATUS AND PROCEDURES

The test equipment is a 1/30 down-scaled of Germany upper plenum test facility (UPTF) simulator with the horizontal length to diameter (L/D) and the riser length to diameter (I/D) ratio were 24 and 8.3, respectively. The rig comprises an RPV, a hot leg, an SG, and also an upper and a lower water tank. Here, the air from the compressor is used to simulate vapor pressure. FIGURE 1 depicts the experimental apparatus. The water from the upper water tank flows through the valve and water flow meter before reaching the SG. The air from RPV flow to SG, via the hot leg, bend, and riser. At the same time, in hot leg countercurrent flow occurs between water and air.

Table 1. Physical properties of the working fluids

Physical properties	Water	Air
Fluid density at 30 ° C (kg/m ³)	996	1.165
Dynamic viscosity at 30 ° C (kg/m. s)	7.97×10^{-4}	1.87×10^{-5}
Surface tension (kg/s ²)	71.97×10^{-3}	-

The visual observations were made on the hot leg and riser using a Phantom high-speed camera. The flooding phenomenon in the hot leg section can be obtained by adjusting the air and water flow rates. The visual data was processed on the basis of MATLAB language according to the procedure described by Widyatama et al. (2018). Here, the conceptual idea involves performing a visual conversion from RGB to grey and comparing it to the background image.

The data are retrieved by adjusting the water flow from the upper water tank to the SG at constant rate while the gas is gradually increased every 15 seconds until onset of flooding occurs. The data from the visualization video is processed in MATLAB and converted to film thickness data in the .XLSX file format, which can be processed in Microsoft EXCEL. Moreover, the MATLAB software was used to obtain scholastic analysis characteristics in the form of the PDF and wavelets analysis.

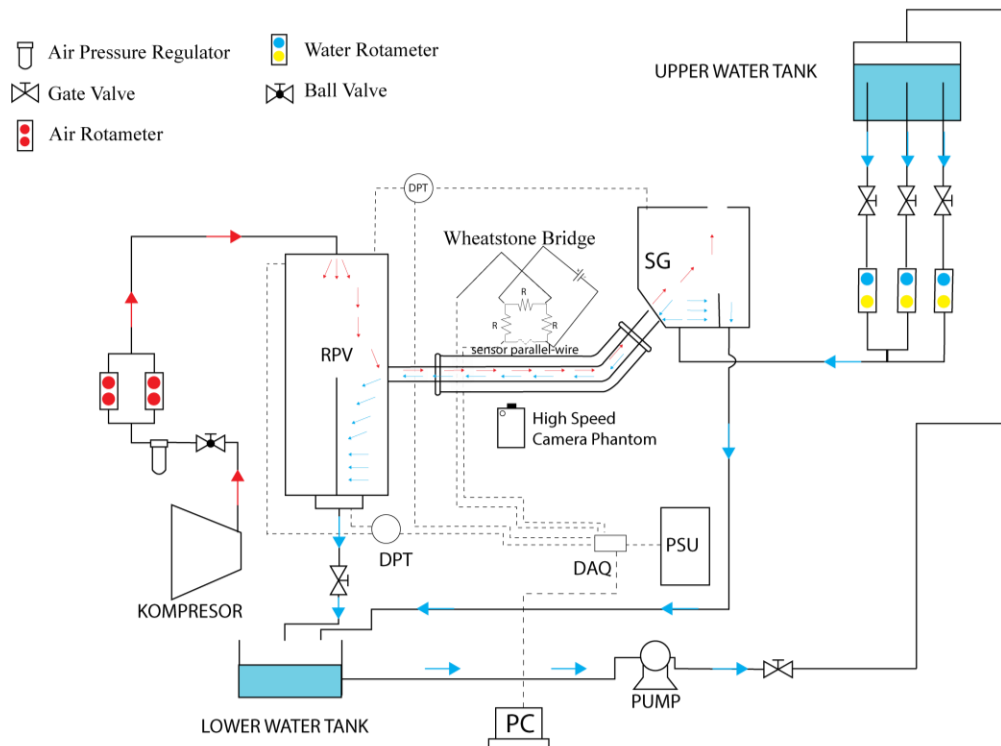


FIGURE 1. PWR simulator scheme.

RESULTS AND DISCUSSIONS

Flooding Mechanism

In this study the flooding mechanisms were described through a close visual observation towards the high-quality photographs. This method of observation was previously reported by Al Issa and Macian (2014), and also Deendarlianto et al. (2008). In the present work, a Phantom Miro Lab310 high-speed camera was employed to visualize the flooding mechanism. The high-speed camera records the hot leg fluid interface. The air flow rate is varied under a constant water superficial velocity of 45 litres per minute (lpm).

Under the condition of $Q_G = 14$ gallon per hour (gph), the detail of flow condition is explained as follows. First, water enters the inlet and flows through the riser. Here, the water flow is accelerated by the gravity. As a result, it creates a supercritical flow in the bend. In this flow condition, a hydraulic jump (HJ) phenomenon is observed at Locus 8 and 9 when $t = 1.36s$. The HJ tends occur before the onset of flooding. This phenomenon is in agreement with those reported by Deendarlianto et al. (2008) in which a hydraulic jump is a transition from subcritical to supercritical flow. After the transition from subcritical to supercritical flow the wavy flow phenomenon appears at Locus 4 and 5 when $t = 2.7s$.

As time progress, the wavy flow induces roll waves at Locus 6 and 7 at $t = 4s$. The roll wave phenomenon initiates a liquid blockage at Locus 8 when $t = 4.05s$ while the churn flow phenomenon was discovered near the riser at Locus 10. The similar phenomenon was reported by Al-Isaa and Macian (2014). Moreover, according to Deendarlianto et al. (2008), the churn flow phenomenon in riser was caused by decreased cross-sectional area for airflow during the onset of flooding. As a result, the air accelerates above the wavy flow, breaks the liquid slug and transforms it into droplets in the SG section.

The phenomena observed under the flow condition of $Q_L = 18$ gph is similar to those observed at $Q_L = 14$ gph. Here, a hydraulic jump was discovered at Locus 7, 8, and 9. Following the appearance of the HJ, a wavy flow developed into a roll wave, resulting in a blockage. The blockage events tend to shift in the horizontal section of the hot leg in the middle (at Locus 5). Additionally, a churn flow pattern was discovered in the riser section.

The HJ phenomenon tends shifting closer to the RPV at a gas discharge rate of 20 gph. The HJ occurs at Locus 6, 7, 8 and 9. Continuing to follow the appearance of HJ, the flow becomes wavy and develops into a roll wave. This roll wave initiates blockage, which results in the onset of flooding. FIGURE 2a and 2b illustrated the visualization and the liquid film fluctuation obtained by image processing technique.

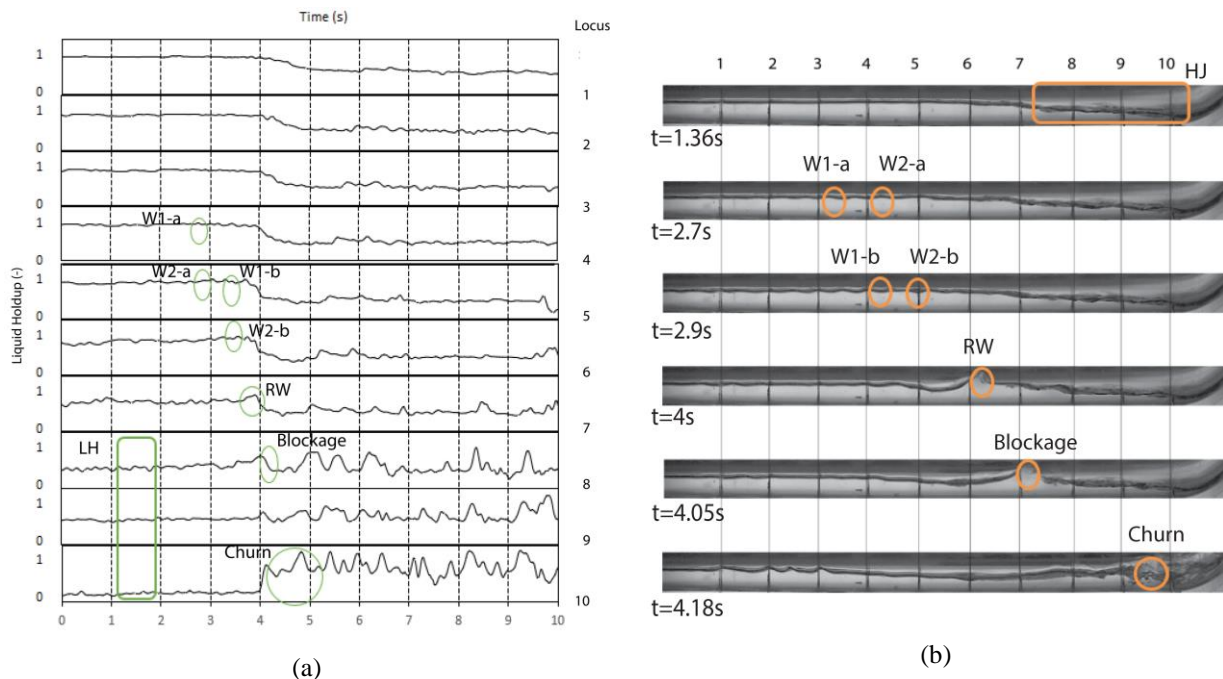


FIGURE 2. (a) The liquid film fluctuation, and (b) flow visualization during the flooding phenomena at $Q_L = 14$ gph.

Stochastic Analysis

FIGURE 4 shows liquid holdup fluctuation and the PDF under the condition of $Q_G = 45$ lpm for various water flow rates at Locus 10. In the PDR regime, the rise in liquid holdup density correlates to the onset of flooding, which develops faster at the greatest water flow for a given gas discharge rate. The multimodal curve demonstrates many dominant liquid film thicknesses, particularly before and after the onset of liquid blockage (flooding). In some regions, the onset of liquid blockage is characterized by a drastic drop in the thickness of the liquid film, whereas in others, it can be indicated by an abrupt increase in, or change in, liquid holdup fluctuations, as illustrated in FIGURE 3. This sudden decrease in liquid holdup is explained by the pressure difference formed by the blockage. Here, one of the indicators of the CCFL regime is a high-pressure difference between the RPV and SG as reported by Deendarlianto et al. (2012).

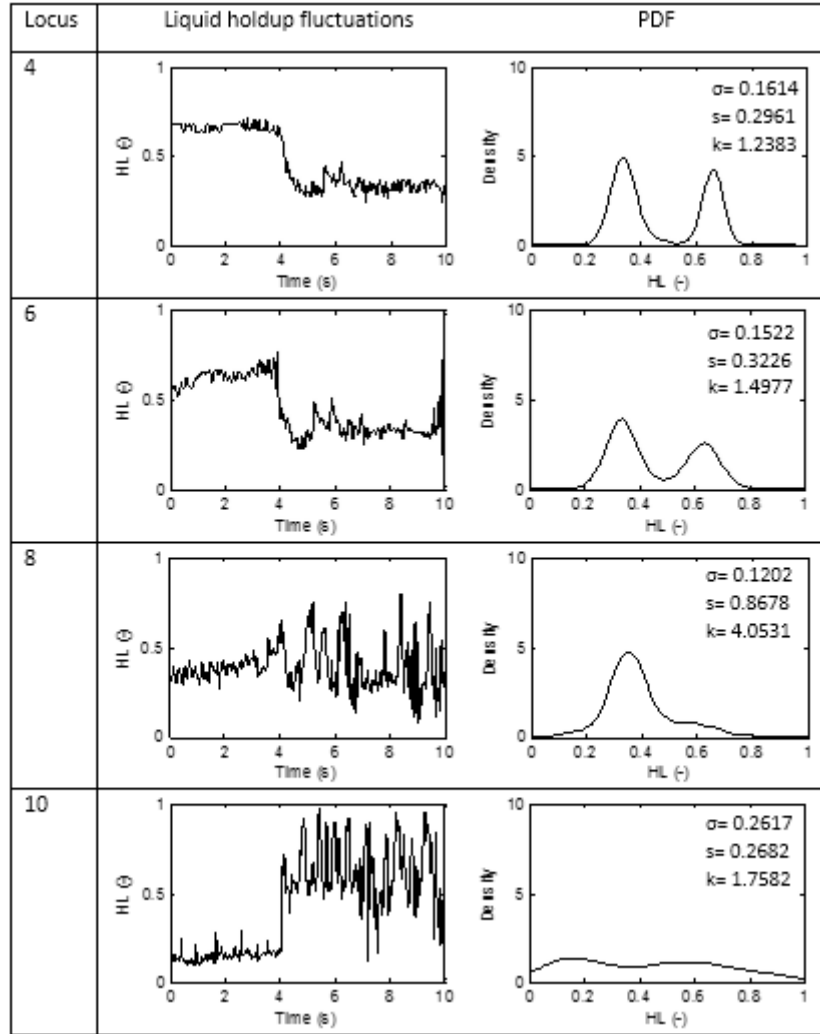


FIGURE 3. Typical liquid holdup fluctuation at $Q_L = 14$ gph and $Q_G = 45$ lpm for various Locus.

According to the PDF graph as illustrated at FIGURE 4, the density tends to increase along with the increase of air flow rate. This implies that the flow with a larger gas flow rate has a more fluctuated liquid holdup. At $Q_G = 14$ lpm, the measured liquid holdup started to exhibit significant fluctuations at $t = 4$ s. Here, the PDF shows twin peaks which indicates that the flow is two-phase flow slug flow. This is explained in further detail in the study that was undertaken by Rodriguez et al. (2020). However, the twin peaks parameters do not directly reflect the two-phase slug flow characteristics because the collecting data includes the process preceding the CCFL. Under the flow condition of $Q_L = 18$ gph, the liquid holdup fluctuates between $t = 0$ -2s. Here, the fluctuation is more significant at t

= 4s. The standard deviation has decreased, and the PDF observed at $Q_L = 14$ gph flow is a twin peak with the same pattern. At $Q_L = 20$ gph, the liquid holdup fluctuated between $t = 0-2s$, more significant than at $Q_L = 18$ gph. However, at $t = 4s$, the liquid holdup fluctuates more. The observed PDF curve is different from the one observed between $Q_L = 14$ gph and $Q_G = 18$ gph, which has a single peak PDF. The increase in the density of liquid holdup fluctuations in the PDR regime indicates that flooding occurs more quickly as water discharge increases for the same gas discharge value as demonstrated by the Wallis curves from previous studies as reported by Navaro (2005), Vallee et al. (2012), and Astyanto et al. (2021).

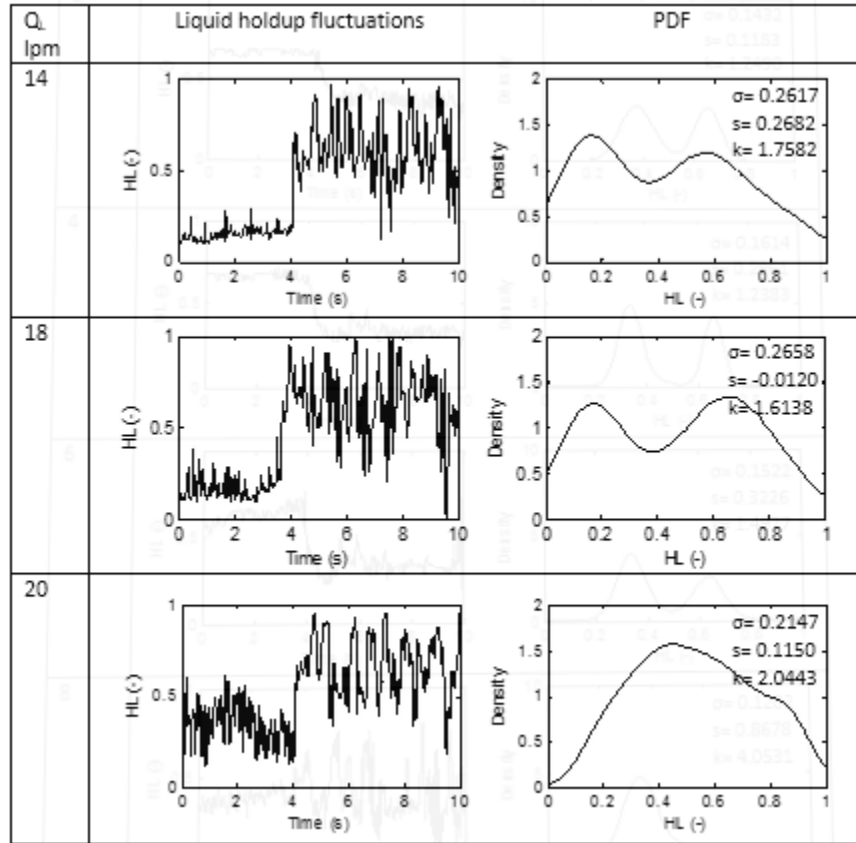


FIGURE 4. Typical liquid holdup fluctuations and the PDF at $Q_G = 45$ lpm for various water flow rates of Locus 10.

The average fluctuation shown in FIGURE 5a follows a generally similar pattern between $Q_L = 14$ gph and $Q_L = 18$ gph, the curve drops from Locus 1 to Locus 2, then remains relatively constant until Locus 7, the fluctuation curve is then distributed from Locus 8 to 10. Meanwhile, $Q_L = 20$ gph resulted a decrease the average fluctuation curve from Locus 1 to 7, then the average fluctuation curve was distributed from Locus 8 to 10. Visual findings indicate that HJ is spread between Locus 7 and 9 and that the commencement of liquid obstruction moves farther from the bend hot leg as water flow increases.

Moreover, FIGURE 5b illustrates the standard deviation (SD) fluctuation. Under flow condition at $Q_L = 14$ gph, there is an increases SD trend from Locus 1 to 5, then the SD tends to distributed from Locus 5 to 10. When the water flow rate increases to 18 gph, the SD increases from Locus 1 to 3, then SD curve is distributed at Locus 3 to 10. Hence at $Q_L = 20$ gph, SD fluctuation tends to increase from Locus 1 to 4 and then distributed from Locus 5 to 10.

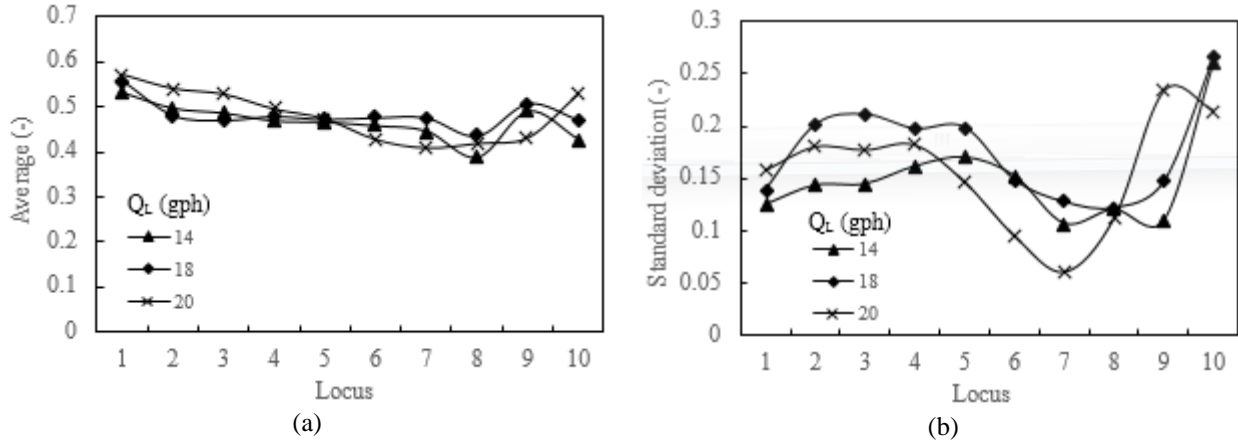


FIGURE 5. (a) Average, and (b) standard deviation of liquid holdup fluctuations at $Q_G = 45$ lpm for various Q_L at Locus 10.

Energy Fluctuation

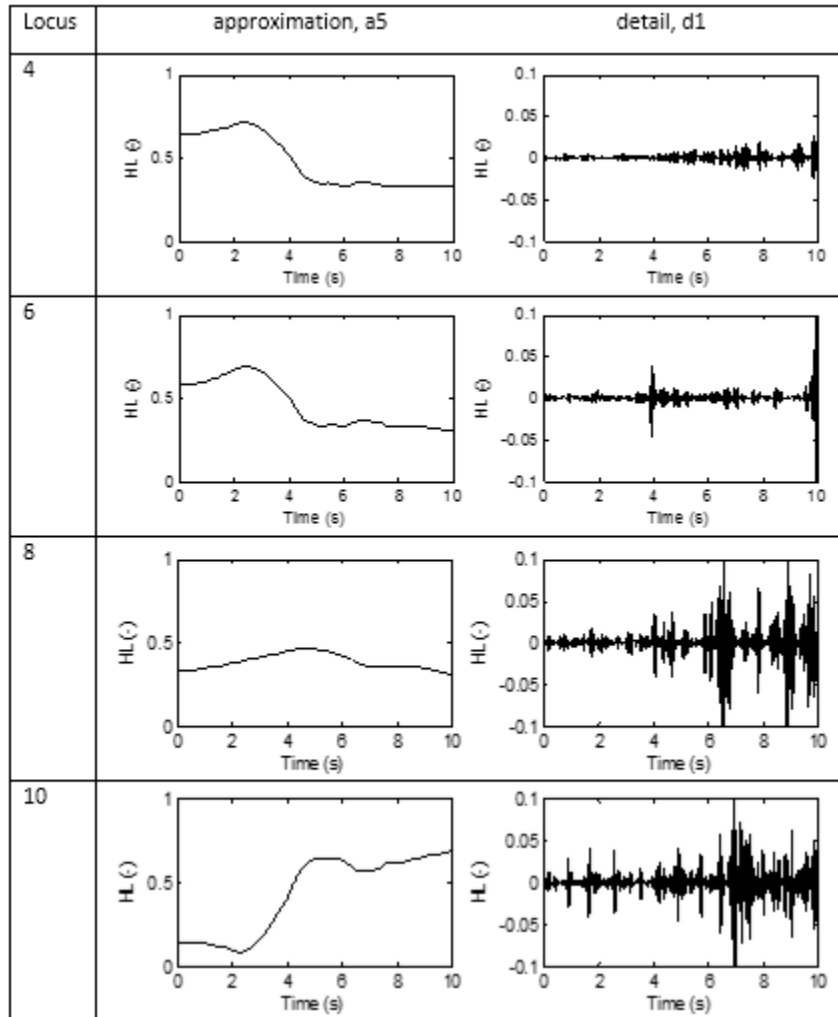


FIGURE 6. Wavelet approximation and detail at $Q_G = 45$ lpm for various water flow rates on Locus 10

In the present study, a discrete wavelet transform from Daubechies 4 family which was previously employed by Jana et al. (2006), and Catrawedarma et al. (2021) was utilized to decompose the original time-series liquid holdup fluctuations into five levels of detail scale. Here, d1 represents the smallest scale detail with the highest frequency, while d1, d3, d4, and d5 corresponds to the lower frequencies. On the other hand, a5 gives the largest-scale approximation.

FIGURE 6 represents the predicted and typical wavelet details for various Locus under flow condition of $Q_G = 45$ lpm and several water flows rates. From the figure it is noticed that at Locus 2, 4, 6 and 8 the liquid holdup fluctuations distribute with the same characteristics. Here the approximation slightly increases from $t = 0$ to $t = 2s$ and then decreases at $t = 4s$. At Locus 8, the approximation value is skewed horizontally. At the Locus 10, the approximation increased from $t = 2s$. In a contrary, the value of detail d1 tends to more fluctuated along with the increased Locus number. In addition, as time progress the detail fluctuations tend to increase.

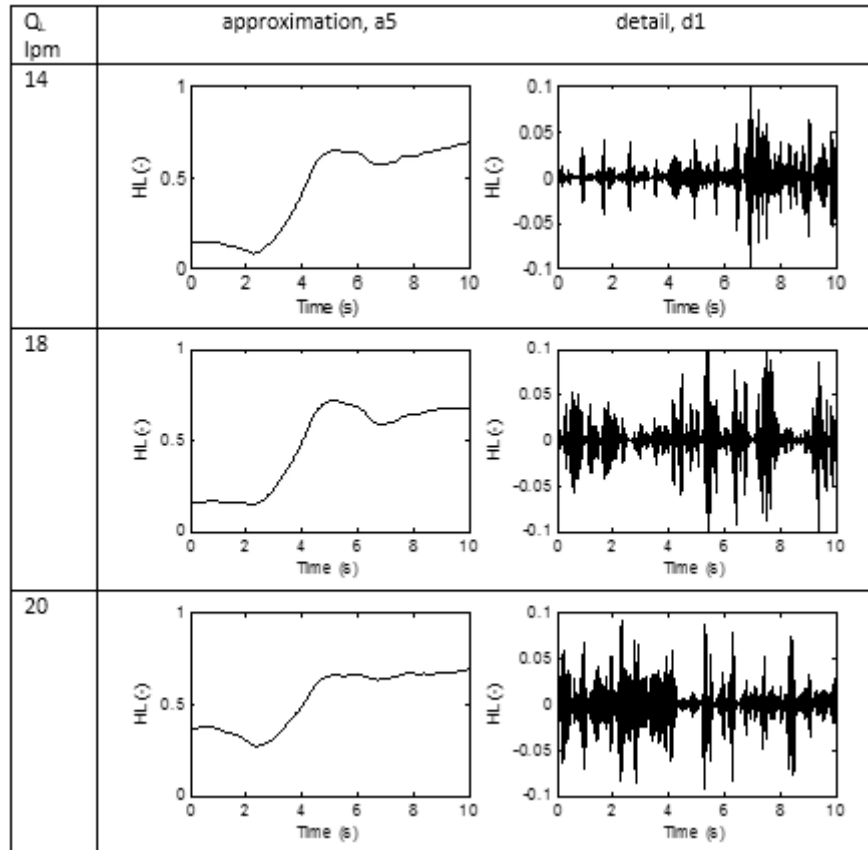


FIGURE 7. Wavelet approximation and detail under $Q_G = 45$ lpm for various water flow rates at Locus 10.

FIGURE 7 illustrates the approximate and typical wavelet details at $Q_G = 45$ lpm for various water flow rates. Here, the approximation for $Q_L = 14, 18$ and 20 lpm shows the same characteristics. Moreover, at $t = 4s$, the approximations increase significantly. An increase in the water flow rate also causes the approximation to increase, while the detail tends to fluctuate as water flow rate increases. Additionally, the wavelet analysis of the fluctuations in FIGURE 8 implies that under flow conditions at $Q_L = 14$ gph, the energy fluctuations tend to increase from d1 to d5. Hence, the fluctuation energy at $Q_L = 18$ gph tends to distribute from d1 to d4. Meanwhile, the fluctuation energy at $Q_L = 20$ gph tends to distribute from d1 to d5.

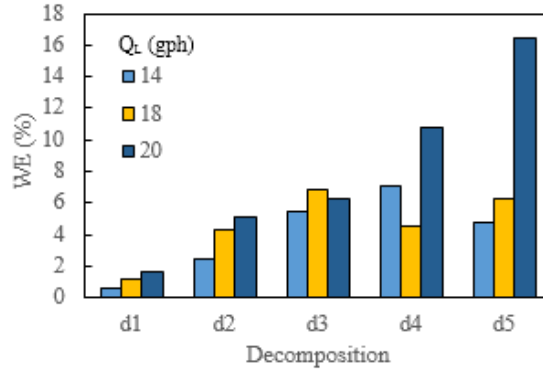


FIGURE 8. Wavelet approximation and detail at $Q_G=45$ lpm for various water flow rates on Locus 10.

FIGURE 9a exhibits a similar trend under flow condition of $Q_L = 14$ and 18 gph. Here, the detail increases from Locus 5 and then the curve distributed at Locus 6 to 10. Under the flow conditions of $Q_L = 20$ gph the detail tends to increase at the Locus 6, the curve is distributed at Locus 7 to 10. On the other hand, the approximation of all water flow discharges reveals a consistent pattern from Locus 1 to 5. Here, the trend shows approximation with relatively stable horizontal line for all Q_L . Moreover, under the flow condition of $Q_L = 14$ gph, the approximation increases at Locus 9. Additionally, at $Q_L = 18$ gph and 20 gph, the approximations increase at the Locus 8. Here, at $Q_L = 20$ gph the approximation tends to fluctuate during the locus shift closer to the bend as illustrated FIGURE 9b.

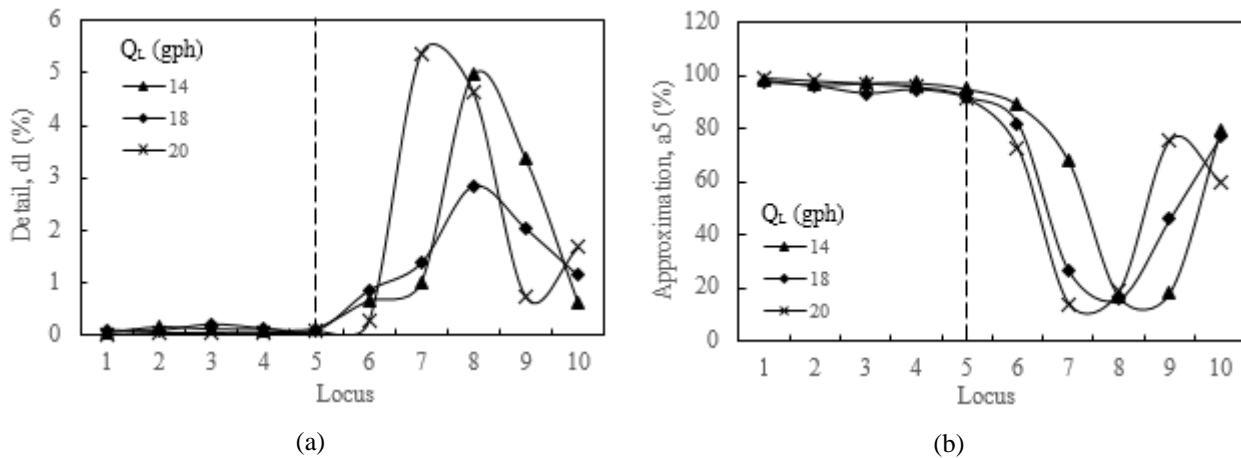


FIGURE 9. Wavelet analysis of (a) detail, d1 and (b) approximation, a5 at $Q_G=45$ lpm for various water flow rates and Locus.

CONCLUSION

The statistical characterization of image processing-based on the liquid film thickness fluctuations during two-phase countercurrent flow limitation (CCFL) on a complex geometry has been investigated. The results to be highlighted are:

1. The flooding mechanism that observed by visual observations and image processing data validation obtained before the flooding process is indicated by a hydraulic jump near the bend area. Over time, a wavy flow appears that moves in the opposite direction of the water flow; the wavy flow then transforms into a roll wave. The roll wave grows over time, closing the entire flow and causing a blockage phenomenon, which is the initiation of onset flooding. A churn flow pattern can be seen after the onset of flooding in the area around the bend.
2. According to stochastic analysis, liquid holdup fluctuations tend to be the same for all water discharges used. Characteristics indicating a tendency for the slope to decrease as the location approaches the bend area, then fluctuates in the area around the bend. Meanwhile, the amplitude of liquid holdup fluctuations follows a consistent pattern with each water discharge.

3. At high flow rates, the energy wavelet shows that the low-frequency group has the highest energy fluctuations, whereas at lower discharges, the energy fluctuations are distributed as the frequency decreases

ACKNOWLEDGMENT

This manuscript was written in terms of academic research in the Laboratory of Fluid Mechanics, Department of Mechanical and Industrial Engineering, Universitas Gadjah Mada to earn Master in Mechanical Engineering title. The authors thank to Kementerian Pendidikan, Kebudayaan, Riset dan Teknologi (KEMENDIKBUD-RISTEK) and Lembaga Pengelola Dana Pendidikan (LPDP) Kementerian Keuangan of Republic Indonesia as the scholarship provider, and the research funder, respectively. We are also grateful to Dr. Apip Badarudin, Dr. I Gusti Ngurah Bagus Catrawedarma and Mr. Setya Wijayanta for the technical supports.

REFERENCES

1. Al Issa, S., & Macian-Juan, R. (2014). Experimental investigation of countercurrent flow limitation (CCFL) in a large-diameter hot-leg geometry: A detailed description of CCFL mechanisms, flow patterns and high-quality HSC imaging of the interfacial structure in a 1/3.9 scale of PWR geometry. *Nuclear Engineering and Design*, 280. <https://doi.org/10.1016/j.nucengdes.2014.08.021>
2. Al Issa, S., & Macian, R. (2011). A review of CCFL phenomenon. *Annals of Nuclear Energy*, 38(9). <https://doi.org/10.1016/j.anucene.2011.04.021>
3. Astyanto, A. H., Rahman, Y., Medha, A. Y. A., Deendarlianto, & Indarto. (2021). Pengaruh Rasio I/D terhadap Permulaan Flooding dan Fluktuasi Voltase Sinyal Tekanan Rezim Flooding pada Geometri Kompleks. *Rekayasa Mesin*, 12(August), 447–457. <https://rekayasamesin.ub.ac.id/index.php/rm/article/view/861>
4. Badarudin, A., Indarto, Deendarlianto, & Setyawan, A. (2016). *Characteristics of the air-water counter current two-phase flow in a 1/30 scale of pressurized water reactor (PWR): Interfacial behavior and CCFL data*. <https://doi.org/10.1063/1.4949303>
5. Badarudin, A., Setyawan, A., Dinaryanto, O., Widyatama, A., Indarto, & Deendarlianto. (2018). Interfacial behavior of the air-water counter-current two-phase flow in a 1/30 scale-down of pressurized water reactor (PWR) hot leg. *Annals of Nuclear Energy*, 116. <https://doi.org/10.1016/j.anucene.2018.03.007>
6. Catrawedarma, I., Deendarlianto, & Indarto. (2021). Statistical Characterization of Flow Structure of Air–water Two-phase Flow in Airlift Pump–Bubble Generator System. *International Journal of Multiphase Flow*, 138. <https://doi.org/10.1016/j.ijmultiphaseflow.2021.103596>
7. Deendarlianto, Höhne, T., Lucas, D., & Vierow, K. (2012). Gas–liquid countercurrent two-phase flow in a PWR hot leg: A comprehensive research review. *Nuclear Engineering and Design*, 243. <https://doi.org/10.1016/j.nucengdes.2011.11.015>
8. Deendarlianto, Vallée, C., Lucas, D., Beyer, M., Pietruske, H., & Carl, H. (2008). Experimental study on the air/water counter-current flow limitation in a model of the hot leg of a pressurized water reactor. *Nuclear Engineering and Design*, 238(12). <https://doi.org/10.1016/j.nucengdes.2008.08.003>
9. Jana, A. K., Das, G., & Das, P. K. (2006). Flow regime identification of two-phase liquid–liquid upflow through vertical pipe. *Chemical Engineering Science*, 61(5). <https://doi.org/10.1016/j.ces.2005.09.001>
10. Navarro, M. A. (2005). Study of countercurrent flow limitation in a horizontal pipe connected to an inclined one. *Nuclear Engineering and Design*, 235(10–12). <https://doi.org/10.1016/j.nucengdes.2005.02.010>
11. Rodrigues, R. L. P., Cozin, C., Naidek, B. P., Marcelino Neto, M. A., da Silva, M. J., & Morales, R. E. M. (2020). Statistical features of the flow evolution in horizontal liquid-gas slug flow. *Experimental Thermal and Fluid Science*, 119. <https://doi.org/10.1016/j.expthermflusci.2020.110203>
12. S. WONGWISES. (1996). FLOODING IN A HORIZONTAL PIPE WITH BEND. *Int. J. Multiphase Flow*, 22, 195–201.
13. Vallée, C., Seidel, T., Lucas, D., Beyer, M., Prasser, H.-M., Pietruske, H., Schütz, P., & Carl, H. (2012). Counter-current flow limitation in a model of the hot leg of a PWR—Comparison between air/water and steam/water experiments. *Nuclear Engineering and Design*, 245. <https://doi.org/10.1016/j.nucengdes.2012.01.001>
14. Widyatama, A., Dinaryanto, O., Indarto, & Deendarlianto. (2018). The development of image processing technique to study the interfacial behavior of air-water slug two-phase flow in horizontal pipes. *Flow Measurement and Instrumentation*, 59. <https://doi.org/10.1016/j.flowmeasinst.2017.12.015>

AIP Conference Proceedings



Volume 2836

THERMOFLUID XII The 12th International Conference on Thermofluids 2021

Yogyakarta, Indonesia • 10–11 November 2021

Editors • Hifni Mukhtar Ariyadi, Indarto, Samsul Kamal,
Harwin Saptoadi and Deendarlianto



Available Online: pubs.aip.org/aip/acp